Fig. 8

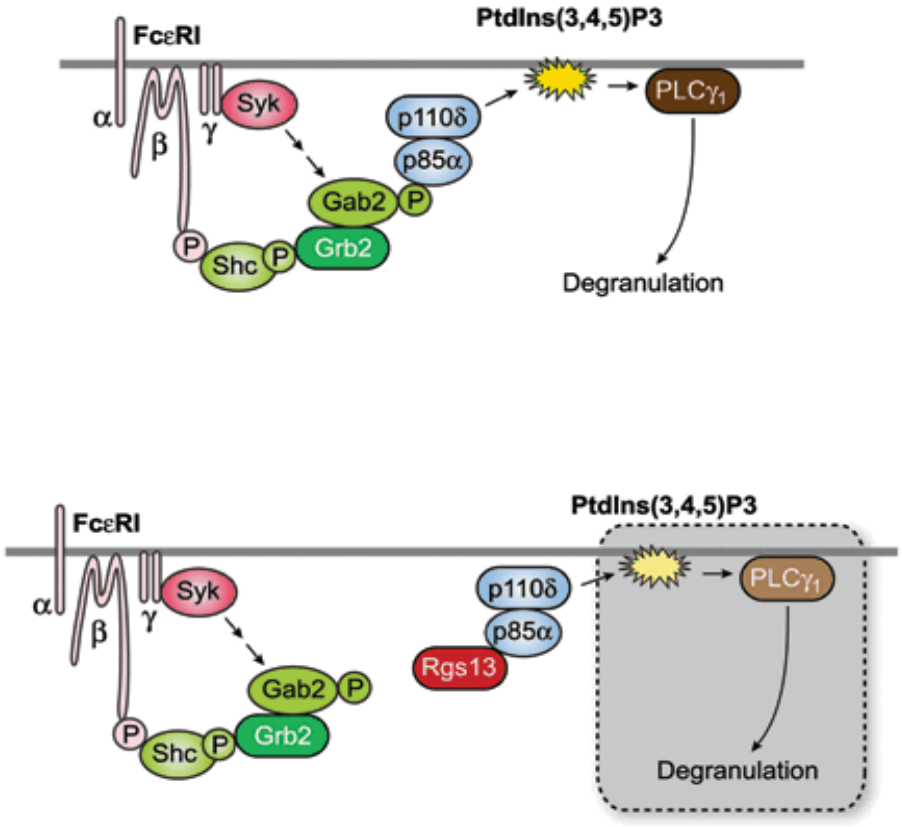

Supplementary Information

Supplementary Fig. 1 Generation of *Rgs13-/-* mice. a, *Rgs13* was targeted by replacing exon 4 with a *LacZ/Neo* cassette as shown. The construct was transfected by electroporation of 129 SvEv embryonic stem (ES) cells. After selection in G418, surviving colonies were expanded, and PCR analysis was performed to identify clones that had undergone homologous recombination. The correctly targeted ES cell lines were microinjected into C57BL/6J host blastocysts. The chimeric mice were generated, which resulted in germline transmission of the disrupted *Rgs13* gene. Chimeras were backcrossed onto the C57BL/6J background for >5 generations and genotypes were born at the expected Mendelian frequency. Homozygous mice were viable and fertile and exhibited no gross phenotypic abnormalities. **b**, Absence of *Rgs13* by RT-PCR. RNA from BMMCs was prepared and analysed for *Rgs13* expression by RT-PCR using primers outlined in the Methods.

Supplementary Fig. 2 β-galactosidase activity identifies physiological Rgs13 expression in mast cells. a, BMMCs were plated on glass coverslips by cytospin, fixed in 0.05% glutaraldehyde and stained with X-gal to analyze β-galactosidase activity. **b,**

Eyeballs were processed similarly and paraffin-embedded for histochemical studies. Giemsa or Toluidine blue staining was used to define tissue histology and MCs (arrowheads). The MC-rich conjunctival fornix is indicated by an arrow.

Supplementary Fig. 3 FcεRI expression on WT and *Rgs13-/-* BMMCs. Cells were stained with anti-DNP IgE and FITC-labeled anti-IgE followed by FACS analysis.

Supplementary Fig. 4 Increased passive systemic anaphylaxis in *Rgs13-/-* mice. Mice were sensitized with 2 μg anti-DNP IgE intravenously followed by next day challenge with 500 μg DNP-HSA containing 0.5% Evans blue intravenously for 1 hr. Dye extravasation was assessed by extraction from organs in formaldehyde and measurement of absorbance at 610 nm. Data represent mean ± S.E.M. from 4-6 mice in each group.

Supplementary Fig. 5 Recombinant RGS13 does not bind unphosphorylated p85α. A pulldown to measure interaction of the two proteins was performed as in Fig. 4c except that p85α was not phosphorylated prior to incubation with RGS13.

Supplementary Fig. 6 Rgs13 deficiency does not affect Ag-evoked p85α phosphorylation. BMMCs from WT or *Rgs13-/-* mice were serum- and cytokine-starved for 24 hrs. prior to Ag stimulation for the indicated times. Lysates were immunoprecipitated with anti-p85α followed by immunoblotting with anti-phosphotyrosine and anti-p85α antibodies.

Supplementary Fig. 7 Deletion of Rgs13 does not affect FcεRI-stimulated Syk or Erk phosphorylation in BMMCs. Cells were sensitized overnight with anti-DNP IgE followed by stimulation with DNP-HSA for the indicated times. Cell lysates were immunoprecipitated with anti-Syk followed by immunoblotting with anti-phosphotyrosine (pTyr) and anti-Syk (**a**) or immunoblotted with anti-phospho Erk1/2 followed by immunoblotting with anti-Erk1 (**b**).

Supplementary Fig. 8 Ag-evoked cytokine production is not affected by deletion of Rgs13 in MCs. BMMCs were sensitized with anti-DNP IgE followed by stimulation with DNP-HSA (30 ng ml^{-1}) for 24 hrs. Supernatants were collected and cytokines measured using Multiplex Luminex Assay. Values represent mean +/- S.D. from a single experiment representative of three independent experiments.

Supplementary Fig. 1

a

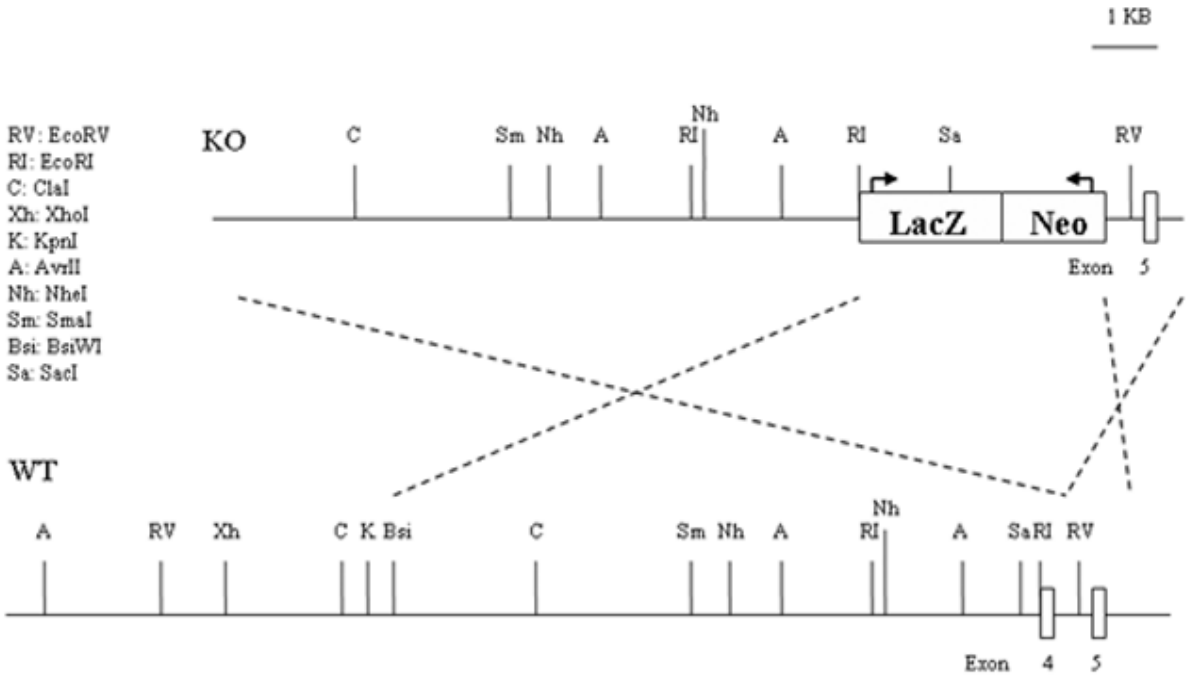

b

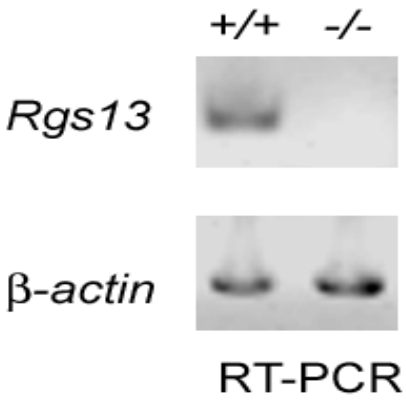

Supplementary Fig. 2

a

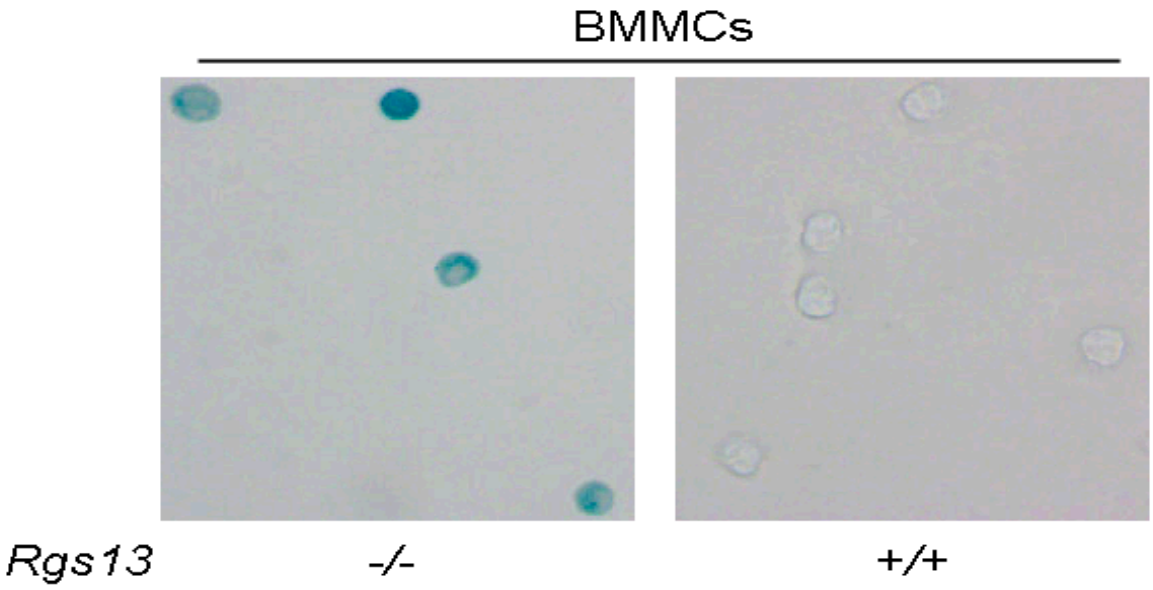

b

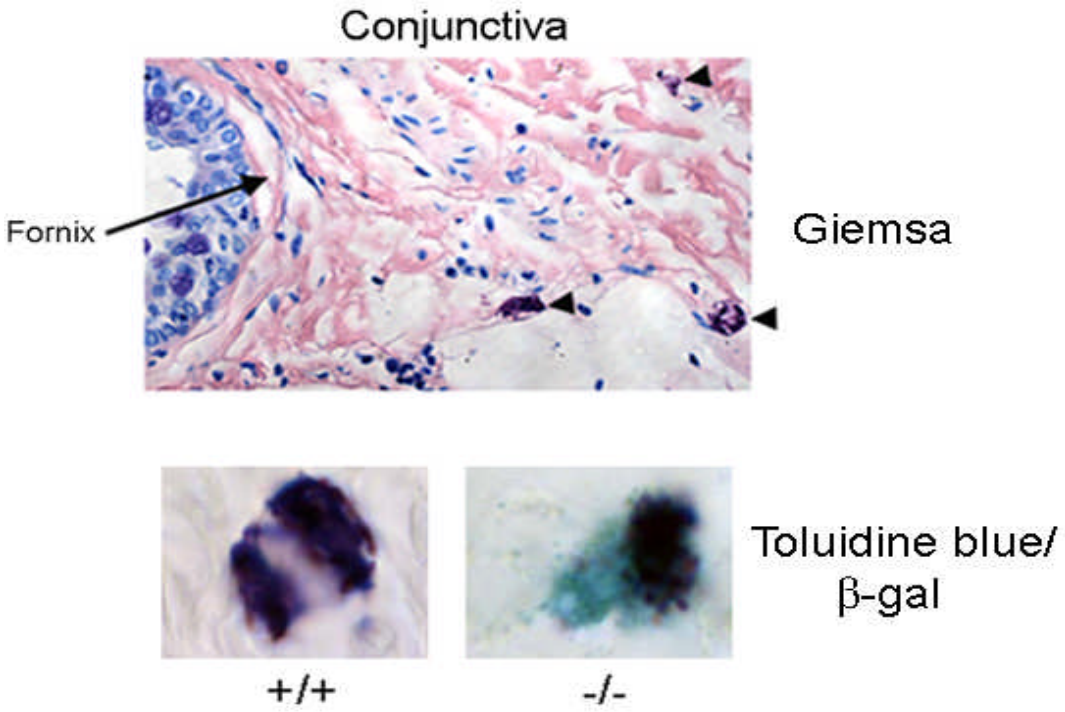

Supplementary Fig. 3

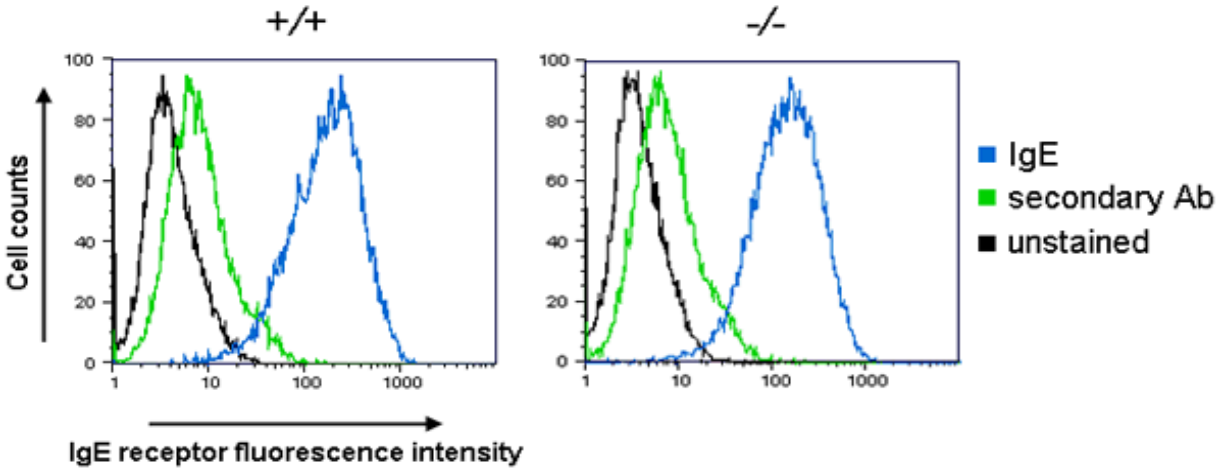

Supplementary Fig. 4

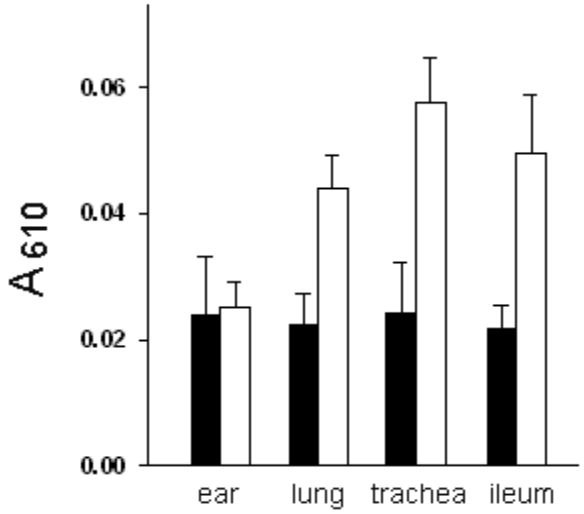

Supplementary Fig. 5

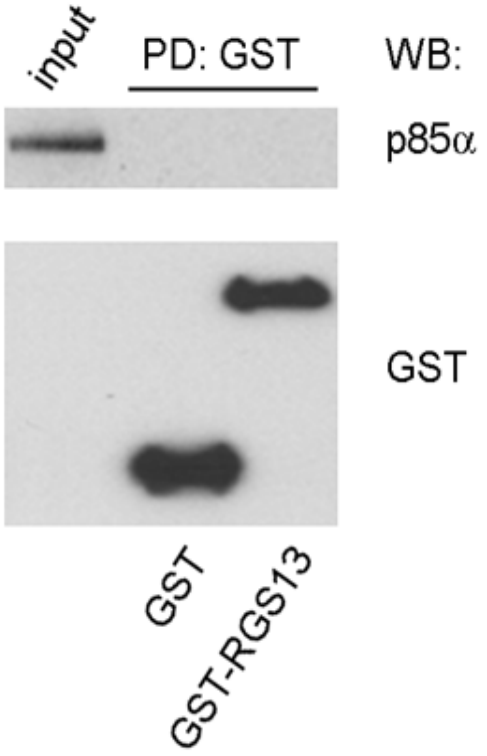

Supplementary Fig. 6

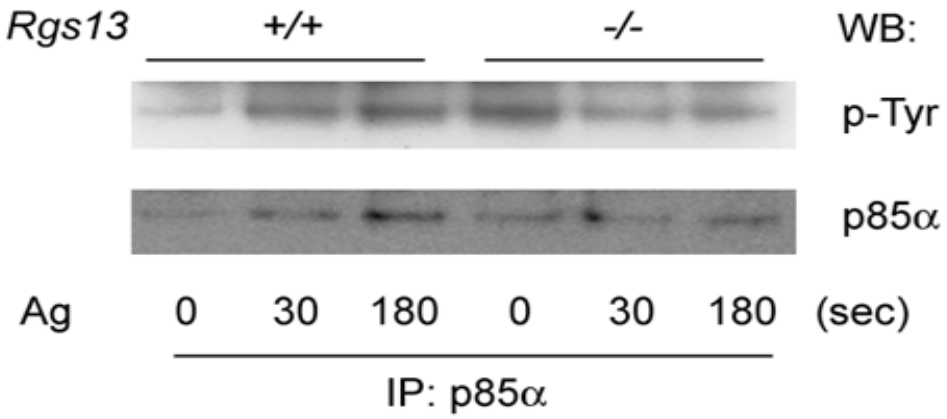

Supplementary Fig. 7

a

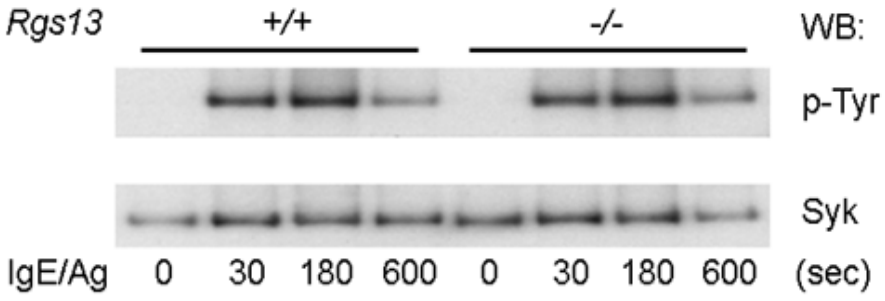

b

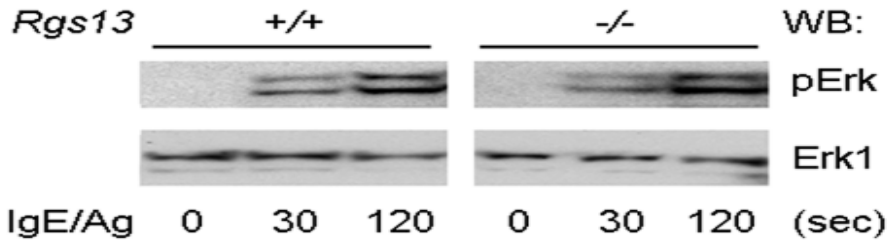

Supplementary Fig. 8